JOURNAL OF CHEMICAL INFORMATION AND MODELING

Article

pubs.acs.org/jcim

SABRE: Ligand/Structure-Based Virtual Screening Approach Using Consensus Molecular-Shape Pattern Recognition

Ning-Ning Wei and Adel Hamza*

University of Kentucky, 789 South Limestone Street, Lexington, Kentucky 40536, United States

ChemVS LLC, Merrick Drive, Lexington, Kentucky 40502, United States and School of life Science and Medicine, Dalian University of Technology, Panjin, LN 124221, China

Supporting Information

ABSTRACT: We present an efficient and rational ligand/structure shape-based virtual screening approach combining our previous ligand shape-based similarity SABRE (*shape-approach-based routines enhanced*) and the 3D shape of the receptor binding site. Our approach exploits the pharmacological preferences of a number of known active ligands to take advantage of the structural diversities and chemical similarities, using a linear combination of weighted molecular shape density. Furthermore, the algorithm generates a consensus molecular-shape pattern recognition that is used to filter and place the candidate structure into the binding pocket. The descriptor pool used to construct the consensus molecular-shape pattern consists of four dimensional (4D) fingerprints generated from the distribution of conformer states available to a molecule and the 3D shapes of a set of active ligands computed using SABRE software. The virtual screening efficiency of SABRE was validated using the Database of Useful Decoys (DUD) and the filtered version (WOMBAT) of 10 DUD targets. The ligand/structure shape-based similarity SABRE algorithm outperforms several other widely used virtual screening methods which uses the data fusion of multiscreening tools (2D and 3D fingerprints) and demonstrates a superior early retrieval rate of active compounds ($EF^{0.1\%}$ = 69.0% and $EF^{1\%}$ = 98.7%) from a large size of ligand database (~95 000 structures). Therefore, our developed similarity approach can be of particular use for identifying active compounds that are similar to reference molecules and predicting activity against other targets (chemogenomics). An academic license of the SABRE program is available on request.

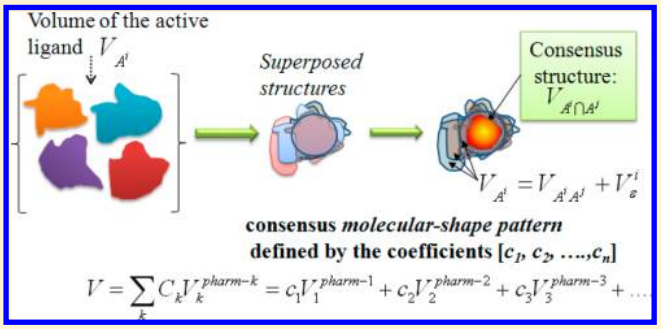

INTRODUCTION

High throughput screening of large compound databases has become increasingly popular technology of finding valuable drug candidates, by applying a wide range of computational methods.[1] There are two fundamental approaches to virtually screen databases for molecules fitting either a known pharmacophore or a three-dimensional (3D) structure of the protein target.[2] While protein-based screening methods require knowledge about the 3D structure of the protein targets,[3] ligand-based approaches typically involve similarity screening by assuming that compounds with similar molecular shapes would have similar properties.[4]

Both structure and ligand based approaches can be applied parallel to virtual screening (VS), but often these approaches are applied in a stepwise filtering approach.[5] The most commonly applied virtual screening methods are pharmacophore identification, molecular docking, and ligand similarity (including 3D shape based) to differentiate actives from inactives based on known data.[6] Simple similarity searching with known active ligands can also be effective.[7]

Despite many reports of successful applications of the ligand shape-based virtual screening methods, serious issues remain unsolved. In general, ligand-based virtual screening typically uses a single known bioactive compound structure and/or its multiple conformations as a query to discover potential active compounds.[8] However, by focusing on only a single bioactive molecule, it is likely that actives with dissimilar structures will be overlooked, leading to a high false-negative rates.[9]

With the increasing availability of crystal structures of multiple, structurally diverse, bioactive ligands for a given protein target, there has been recent interest in the use of multiple template ligands in virtual screening project.[10] Indeed, larger compounds may be able to bind even tighter to a protein by presenting a larger surface and more interaction spots to the target. Conversely, smaller molecules are generally favorable when searching for small lead structure cores with high potential for optimization by medicinal chemistry approaches. Hence, considering multiple compounds of distinct shapes employing the data fusion method may be favorable for shape-based virtual screening.[11]

Received: September 24, 2013
Published: December 12, 2013

   dx.doi.org/10.1021/ci4005496 | *J. Chem. Inf. Model.* 2014, 54, 338−346

The recent comparative studies of well-established ligand and docking-based approaches have consistent conclusion that shape-based ligand screening could yield a markedly better performance than protein docking schemes.[11c,12]

Although the development of molecular docking methods is in progress over the last few decades, the accuracy of modern methods is still far from realistic. Indeed, the objective of any docking method is to find the best candidate ligands, i.e., those with the highest binding affinity, in the smallest possible list to be assayed. With molecular dynamics or Monte Carlo simulations, it is theoretically possible to rigorously evaluate the binding energy of a ligand. However, these methods are time-consuming to be used for the screening of large databases. Therefore, the development of theory and practical application is still a challenge.

We have recently described two approaches that can enhance the effectiveness of the shape based virtual screening. We reported an efficient 3D shape-based similarity algorithm including an effective 3D shape fitting procedure and a robust scoring function HWZ score.[12b] Subsequently, we improved the virtual screening algorithm using an enhanced molecular shape-density model.[12c] Examples of successful applications using SABRE program; see ref 13.

In this paper, we report further developments of these two approaches. The method implemented in the new version of SABRE program combines the ligand and structure shape-based virtual screening approaches. We first present a rational and efficient method that takes a different approach to the computational identification of molecular recognition process. Then, we investigate the impact of the protein binding cavity on the accuracy of the ligand shape-based virtual screening and analyze the possible gain in performance by using the enhanced molecular shape-density model.

Our algorithm is unique in that it takes advantage of the pharmacophoric structural features of known active ligands to generate a consensus molecular-shape pattern recognition that is used to filter and place the candidate structure into the binding pocket.

Finally, we benchmark and analyze the performance of the novel ligand/structure shape-based virtual screening approach using the Database of Useful Decoys (DUD).[14] Furthermore, the results show that the proposed method outperform the ligand shape-based virtual screening using data fusion of multi screening tools, as well as protein docking screening with a single conformation, yielding superior early retrieval rates of active compounds.

METHODS

The overall algorithm of the shape-based ligand similarity screening SABRE (*shape-approach-based routines enhanced*) has been described in our previous work.[12b,c] Briefly, the shape-based virtual screening method takes into account both the structural diversity of each active ligand and the developed scoring HWZ function providing reasonable ranking of compounds. The specific point of our approach exploits the pharmacological preferences from a number of known active ligands to take advantage of the structural and chemical similarities using a weighted molecular shape density of the pharmacophoric groups. The ligand/structure shape-fitting procedure used in the algorithm is achieved by matching the candidate structures in the database with "*substructures*" of the binding active ligand (query), instead of the entire structure of the query and the shape-fitted structures are ranked using the scoring HWZ function. The virtual screening includes two stages: (i) calculation of the optimal coefficients of the shape-density function using a set of known active ligands and (ii) utilization of the optimal coefficients during the automated ligand/receptor shape fitting procedure of the candidate compounds whose activity is unknown.

The active structures are recognized by the way they complement the shape of the binding site and by the recognition of differences in molecular-shape pattern between the active and decoy molecules of the test data set.

Molecular Shape-Density Model. As suggested by Grant et al.,[15] the molecular shape-density of a ligand is calculated using the Gaussian function, in which each atom i with coordinates $\mathbf{R}_i = (X_i, Y_i, Z_i)$ is given by a spherical Gaussian:[16] Gaussian functions are fundamentally smooth because they are infinitely differentiable. Numerical optimization methods either implicitly or explicitly assume continuous smooth functions, and while they are often robust enough to deal with small discontinuities, their performance improves when used with truly smooth functions.[16a]

$$\rho_i(\mathbf{r}) = p_i \exp(-\alpha_i(\mathbf{r} - \mathbf{R}_i)^2) \quad \text{in which } \alpha_i = \pi\left(\frac{3p_i}{4\pi\sigma_i^3}\right)^{2/3} \tag{1}$$

where the amplitude is set to $p_i = 2\sqrt{2}$, and the decay factor α_i is calculated from p_i and σ_i is the van der Waals radius of the atom i.[15a] The molecular shape-density is the sum of all individual atomic densities. The molecular shape density suggested by Mezey et al. is given by

$$D(\vec{r}) = \sum_{i=1}^{n} \rho_i(\vec{r}) \tag{2}$$

And the molecular volume V of the ligand is defined by Grant and Pickup:[17]

$$V = \sum_{i=1}^{n} \int \mathrm{d}\mathbf{r}\, \rho_i(\mathbf{r}) \tag{3}$$

The shape-density model implemented in SABRE is improved by adding the C_k coefficients to the amplitude of the Gaussian function.[12c] The coefficients can be weighted according to some physicochemical property of the atoms.[18] Recently, Yan et al. have described a similar approach, in which the molecular shape density is represented as a linear combination of weighted atomic Gaussian functions.[19]

In the SABRE algorithm, the molecular shape density is the sum of all individual weighted pharmacophore densities, in which the C_k coefficient is interpreted as the weight of the pharmacophoric group k in the structure.

According to eq 3, the molecular volume is rewritten as

$$V = \sum_{k} C_k \sum_{i} \int \mathrm{d}\mathbf{r}\, \rho_{ki}(\mathbf{r}) \tag{4}$$

The basic assumption of our enhanced shape-based similarity approach is that molecules of shape and chemistry comparable to known active compounds (query structure + template structures) have a significant probability of also having same weight for the Gaussian functions of the overlapped pharmacophoric groups.

Then we can rewrite eq 4 as

dx.doi.org/10.1021/ci4005496 | J. Chem. Inf. Model. 2014, 54, 338−346

$$V = \sum_k C_k V_k^{\text{pharm-}k} = c_1 V_1^{\text{pharm-1}} + c_2 V_2^{\text{pharm-2}} + c_3 V_3^{\text{pharm-3}} + \ldots$$

where $V_K^{\text{pharm-}k} = \sum_i \int \mathrm{d}\mathbf{r}\ \rho_{ki}(\mathbf{r})$ is the partial volume of the pharmacophoric group k and defined as a linear combination of atomic Gaussian functions (eq 1).

The volume overlap V_{AB} of two molecules A and B is defined as

$$V_{AB} = \langle V_A | V_B \rangle = \sum_{i\in A} \sum_{j\in B} C_i C_j \exp\left(-\frac{\alpha_i \alpha_j d_{ij}^{\ 2}}{\alpha_i + \alpha_j}\right)\left(\frac{\pi}{\alpha_i + \alpha_j}\right)^{3/2} \quad (5)$$

where i and j refer to atoms in molecules A and B, respectively, and d_{ij} is the distance between atoms i and j. In order to perform the superposition between a pair of molecules, the algorithm translates the molecular shape-density of the moving molecule (B) to that of the query structure (molecule A) and then searches for the rotation that minimizes the "distance" between the corresponding pairs of spherical Gaussian functions.

Identification of the Consensus Molecular-Shape Pattern. The optimal C_k coefficient defined by eq 4 is determined by iteratively adjusting the coefficient of the pharmacophoric group k using the query and a set of known active ligand structures.

Thus, the superimposition of two active ligands A^i (with volume V_{A^i}) and A^j (with volume V_{A^j}) is scored according to the shape-density overlap $V_{A^iA^j}$. The commonly occupied volume $V_{A^i \cap A^j}$ is normalized by the total volume $V_{A^i \cup A^j}$ to arrive at the Tanimoto-like shape similarity:

$$T^{ij} = \frac{V_{A^i \cap A^j}}{V_{A^i \cup A^j}} \quad (6)$$

A schematic view is displayed in Figure 1a.The weighted volume of the two active ligands A^i and A^j can be described as

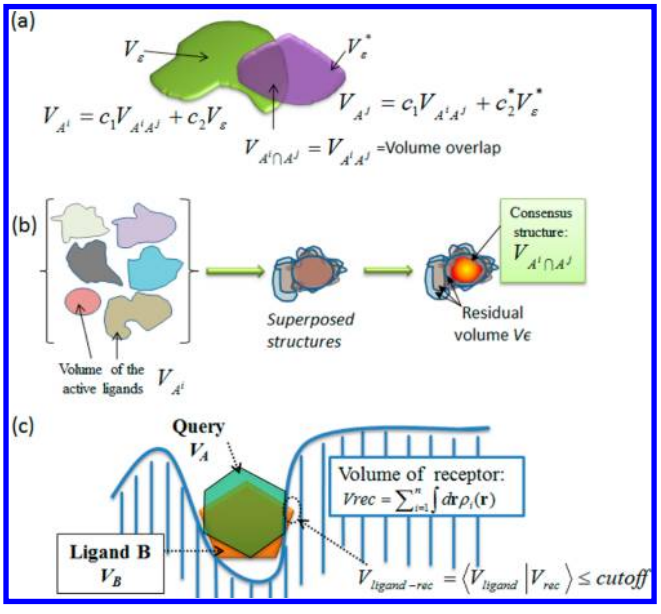

Figure 1. Schematic view of the enhanced shape-based similarity approach (a and b) and the ligand docking approach (c).

$$V_{A^i} = V_{A^iA^j} + V_\varepsilon^i \quad \text{with } V_{A^iA^j} = c_1 V_1^{\text{pharm-1}} + c_2 V_3^{\text{pharm-2}} + c_3 V_3^{\text{pharm-3}} + \ldots \quad (7)$$

$$V_{A^j} = V_{A^jA^i} + V_\varepsilon^j \quad \text{with } V_{A^jA^i} = c_1^* V_1^{\text{pharm-1}*} + c_2^* V_2^{\text{pharm-2}*} + c_3^* V_3^{\text{pharm-3}*} + \quad (8)$$

where V_ε^i (or V_ε^j) is the residual volume of the active ligands i (or j) (Figure 1a) and the $V_{A^iA^j}$ and $V_{A^jA^i}$ terms are the optimal volume overlap of the linear combination of weighted pharmacophoric groups of A^i with A^j.

The similarity of two structures is defined by the Tanimoto equation.

$$T^{ij} = \frac{V_{A^i \cap A^j}}{V_{A^i \cup A^j}} = \frac{V_{A^iA^j}}{(V_{A^iA^j} + V_\varepsilon^i) + (V_{A^jA^i} + V_\varepsilon^j) - V_{A^iA^j}} \quad (9)$$

And, rewritten as

$$T^{ij} = \frac{V_{A^iA^j}}{(V_{A^jA^i} + V_\varepsilon^i + V_\varepsilon^j)} \quad (10)$$

The maximal similarity of the two structures is reached after optimization of the coefficients in eq 4 and defined as

$$T^{ij} = \frac{V_{A^iA^j}}{(V_{A^jA^i} + V_\varepsilon^i + V_\varepsilon^j)} = 1$$

when

- The coefficients of the residual volumes V_ε^i and V_ε^j converge to zero.
- The coefficients of the overlap volume described by the eqs 7 and 8 satisfy the following condition:

$$V_{A^iA^j} = V_{A^jA^i}$$

or

$$c_1 V_1^{\text{pharm-1}} + c_2 V_2^{\text{pharm-2}} + c_3 V_3^{\text{pharm-3}} + \ldots = c_1^* V_1^{\text{pharm-1}*} + c_2^* V_2^{\text{pharm-2}*} + c_3^* V_3^{\text{pharm-3}*} + \ldots$$

For a set of N active ligands (Figure 1b), the optimal coefficients are obtained when the Tanimoto function T^{ij} of each pair of ligands i and j reaches the highest score and are equal.

$$T^{12} = T^{13} = \ldots = T^{1N} = \ldots = T^{(N-1)N}$$

or

$$V_{A^1A^2} = V_{A^1A^3} = V_{A^2A^3} = \ldots = V_{A^{N-1}A^N}$$

and the residual volume V_ε of each active ligand converge to zero.

As a result, we observe that the shape of the ligand is defined as a linear combination of weighted Gaussian functions of the pharmacophoric groups. The algorithm builds a consensus *molecular-shape pattern* defined by the coefficients $[c_1, c_2, \ldots, c_n]$ using a set of active ligands, in which the maximal diversity of chemotypes is taking into account during the screening of the database. These coefficients correspond to the active ligands *signature* of the specific binding target.[12c]

Shape-Fitting Procedure. The approach presented here is a modified version of that proposed by Grant and Pickup.[15a] They observed that replacing atomic hard-sphere functions with Gaussians allowed analytically tractable calculation of

dx.doi.org/10.1021/ci4005496 | J. Chem. Inf. Model. 2014, 54, 338−346

volumes and areas of small molecules. The Gaussian scoring function was proposed by McGann and co-workers as a useful prefilter tool.[20]

The basic idea is that the binding mode of the crystallized ligand structure (query) with specific conformation strongly predetermines the orientation of the candidate molecules and contributes intrinsically to the docking score of active ligands. During the shape fitting, the query structure is placed into a grid box encompassing all active-site atoms of the receptor. The volume of the receptor is created using the smooth Gaussian function defined by eqs 1 and 3 (Figure 1c). The ligand fitting strategy exhaustively explores all possible positions of each candidate ligand in the binding site and generally focused upon two parameters—shape and optimization. Several criteria are typically used to evaluate accuracy of a docking method. First, the accuracy of a putative ligand's pose in a protein−ligand complex.[21]

The initial pose generated by SABRE is determined by shape fitting the candidate ligand B to the binding structure (query A). This prefiltered pose significantly reduces the search space usually explored by docking algorithms. Two optimization filters are subsequently processed:

First, the optimal ligand pose is reached for the highest value of the Gaussian docking function (eq 11). The Gaussian docking function N originally suggested by Grant and Pickup is a summation of pairwise interactions $N_{i,j}$ between the candidate ligand and protein atoms.[15a,17] The pairwise interaction of atoms i and j is defined as

$$N_{i,j}(d_{i,j}) = [1 + \xi({d_{i,j}}^2 - {D_{i,j}}^2)]\exp(-\xi({d_{i,j}}^2 - {D_{i,j}}^2)) \quad (11)$$

with

$$\xi = \frac{\kappa}{({R_i}^2 + {R_j}^2)} \quad \text{and} \quad D_{i,j} = R_i + R_j$$

The total interaction, N, between a set of ligand atoms B and a set of receptor atoms is

$$N = \sum_{i \in B} \sum_{j \in \text{receptor}} N_{i,j} \quad (12)$$

where radii R_i and R_j are the radii of atoms i and j, respectively, and $d_{i,j}$ is the distance between the two atom centers. The parameter κ is a freely adjustable parameter and controls the distribution of the Gaussian function.

Equation 12 shows that the interior of the receptor (protein) is a favorable region for the ligand atoms since there are more atoms making surface contacts. Thus, to avoid the unfavorable atomic clashes between the ligand and receptors atoms, a penalty term is defined as

$$V_{\text{ligand-receptor}} = \langle V_{\text{ligand}} | V_{\text{receptor}} \rangle \leq \text{cutoff} \quad (13)$$

The cutoff value represents the volume overlap limit (degree of interpenetrating) tolerated between the ligand and receptor atoms.

The pose ensemble is then filtered to first reject poses that do not have sufficient shape complementarily with the active site of the receptor (eq 13).

Finally, the Gaussian docking function is described as

$$N = \sum_{i \in B} \sum_{j \in \text{receptor}} N_{i,j} \quad \text{if } V_{\text{ligand-receptor}} \leq \text{cutoff}$$

$$N = 0 \quad \text{if } V_{\text{ligand-receptor}} > \text{cutoff}$$

Second, the accuracy of the virtual screening method where active ligands must be separated from inactive ones:[22]

In SABRE approach, the pose of each candidate ligand with the highest N score is selected and ranked using the HWZ scoring function.[12b]

Validation. For convenience, the ligand-based screening method is named SABRE$^{\text{Lig}}$,[12b] and the current ligand/structure-based screening method is named SABRE$^{\text{Lig-Rec}}$. The validation of SABRE$^{\text{Lig-Rec}}$ was based on an appropriate use of the DUD database[22a] of annotated active compounds and decoys. The DUD is a publicly available virtual screening test database and is the second data set.[23] We have used two data set sources, referred to as database-**1** and database-**2**.

The database-**1** is a subset of DUD consisting of 10 DUD data sets. Good and Opera filtered the DUD data set for lead likeness and then clustered the results on the basis of reduced graph representation.[24] Cheeseright et al. suggest using a subset of 13 targets with more than 15 clusters.[25] Since these have the greatest difference between actives, they should prove more suitable for ligand-based screening methods, and these targets are therefore used in this study. Of these 13 targets, three were excluded due to a homology model (PDGFrb) or problems with broken or missing ligands in the crystal structure (CDK2, VEGFr2).[26]

Database-**1** was downloaded from Web site (http://dud.docking.org/jahn/).[14] The ratio of the number of decoys to the number of active ligands was fixed to 36, in order to be consistent with the ratio used in the previous virtual screening tests (Table 1).[27]

Table 1. Protein Targets Used for the Virtual Screening Test

PDB code	abbreviation	protein target	number of active compounds	number of decoys
1O86	ACE	angiotensin-converting enzyme	49	1764
1EVE	AChE	acetylcholinesterase	105	3780
1CX2	COX-2	cyclooxygenase 2	348	12528
1M17	EGFr	epidermal growth factor receptor	444	15984
1F0R	FXa	factor Xa	142	5112
1RT1	HIVRT	HIV reverse transcriptase	40	1440
1P44	InhA	enoyl ACP reductase	85	3060
1KV2	P38 MAP	P38 mitogen activated protein kinase	256	9216
1XP0	PDE5	phosphodiesterase 5	51	1836
2SRC	SRC	tyrosine kinase	155	5580

Database-**2** was based on the same active ligands and targets of the database-**1** but with the full collection of decoys from all 10 DUD data sets. We decided to use the entire DUD database of decoys for our virtual screening test in order to reflect a real screening scenario. Database-**2** consists of a total of 95171 decoy structures.

To evaluate the effectiveness of the virtual screening approach, we used the previously generated[12b,c] multiple conformations of each ligand (active or decoy) of the 10

dx.doi.org/10.1021/ci4005496 | J. Chem. Inf. Model. 2014, 54, 338−346

Table 2. AUC Values for the 10 Targets of the DUD Database Using Different Virtual Screening Methods[a]

target	SABRE^{Lig}	SABRE$^{Lig-Rec}$	ShaEP[b]	ROCS[b]	CF[b]	FieldScreen[b]
ACE	0.92	0.93 (0.71)	0.58	0.76	0.88	0.67
AChE	0.87	0.88 (0.70)	0.77	0.75	0.66	0.76
COX-2	0.87	0.87 (0.69)	0.61	0.68	0.47	0.92
EGFr	0.73	0.75 (0.60)	0.37	0.62	0.5	0.84
FXa	0.89	0.89 (0.72)	0.76	0.52	0.47	0.74
HIVRT	0.76	0.78 (0.63)	0.71	0.62	0.61	0.70
InhA	0.69	0.72 (0.49)	0.71	0.69	0.75	0.71
P38MAP	0.71	0.72 (0.52)	0.65	0.43	0.43	0.33
PDE5	0.80	0.81 (0.60)	0.63	0.52	0.5	0.66
SRC	0.82	0.83 (0.63)	0.48	0.47	0.84	0.45
average	**0.81**	**0.82 (0.63)**	**0.63**	**0.61**	**0.61**	**0.68**
stand. dev.	0.08	0.07 (0.08)	0.13	0.12	0.16	0.17

[a]The minimum AUC value for each target using SABRE$^{Lig-Rec}$ is reported in parentheses. [b]Reference 30.

targets in the DUD. For each target, the structure of the crystallized ligand was used as query.

Evaluation of the Virtual Screening Efficiency. The effectiveness of the virtual screening was evaluated using the metric enrichment factor (EF), eq 7, at a given percentage of the database screened.[28]

$$EF^{x\%} = \frac{Hits^{x\%}_{selected}/N^{x\%}_{selected}}{Hits_{total}/N_{total}} \quad (14)$$

where $Hits^{x\%}_{selected}$ is the number of hits (active ligands) found at top x% of the database screened, $N^{x\%}_{selected}$ is the number of compounds screened at top x% of the database, $Hits_{total}$ is the number of active ligands in entire database, and N_{total} is the number of compounds in entire database. The efficiency metric was computed using the enrichment factor $EF^{x\%}$ at 1%, 5%, and 10% for each of the 10 DUD targets.

The area under the ROC (*receiver operator characteristic*) curve (AUC) represents another descriptor for virtual screening performance and is calculated as the sum of all rectangles formed by the sensitivity (Se) and specificity (1 − Sp) values for different thresholds.[29] The sensitivity (Se) and specificity (Sp) are defined as

$$Se = \frac{TP}{TP + FN} \qquad Sp = \frac{TN}{TN + FP} \quad (15)$$

where TP represents the number of correctly identified actives (true positives), TN, the number of correctly identified inactives (true negatives), FP, the number of inactives incorrectly predicted as actives (false positives), and FN, the number of actives incorrectly predicted to be inactive (false negatives). The AUC of a ROC plot gives an objective measure of query performance which is essentially independent of the actual number of positive and negative instances. For the ideal distributions of actives and decoys, an AUC value of 1 would be obtained; completely random distributions would lead to an AUC value of 0.5.

To test the robustness of our structure based virtual screening approach SABRE$^{Lig-Rec}$, we decided to screen 8 times each target using different sets of five randomly selected active ligands (as template) and report the lowest and highest performances (ROC AUC value) for each target.

RESULTS AND DISCUSSION

This report extends our previous ligand shape-based screening method implemented in SABRE program.[12b] As described in Methods section, the coefficients have been first optimized using a set of five randomly selected active structures for each target of the DUD database. The virtual screening was carried out for multiple times using the structure of the crystallized ligand as query and different sets of active ligands. In the following study, our intention is not to promote a certain program as being superior to another one, but rather like to point out the relations between our developed ligand and structure shape-based virtual screening algorithms. We are convinced that the best computational performance relies on the combination of an ensemble of these two approaches. To examine the performance and effectiveness of the enhanced shape-based screening method, we have analyzed the results using two different indicators, including area under the ROC curve (AUC) and enrichment factor EF.

Performance of SABRE Using the AUC Metric. The performance of the structure based screening SABRE$^{Lig-Rec}$ was first compared to the ligand based screening SABRE^{Lig} [12b] using the 10 targets of the DUD database (Table 1). The average ⟨AUC⟩ value for the 10 DUD targets, using the best performing set of five active ligands, was 0.82 ± 0.07 and 0.81 ± 0.08 using SABRE$^{Lig-Rec}$ and SABRE^{Lig}, respectively. SABRE$^{Lig-Rec}$ obtained an AUC ≥ 0.8 for 6 targets and 0.8 > AUC ≥ 0.5 for 4 targets and did not "fail" for any of the screened 10 targets.

It is interesting to note that the constraints generated by the shape of the receptor improved the performance of the screening by AUC ∼ 1.2%. While this enhancement is small, a detailed analysis of the AUC values obtained for individual target also reveals an overall superior performance using SABRE$^{Lig-Rec}$ method. Finally, some of the results presented in Table 2, e.g. those for InhA, suggest that adding the shape of the receptor may provide additional accuracy. These results highlight the utility of the fast shape-based filter to remove compounds that cannot fit into the target protein's binding site and then ranking the remaining compounds using the ligand shape-based algorithm. For example, Figure 2 displays the predicted shape fitting of two active ligands in the catalytic domain (active site) of human PDE5 target (PDB: 1XP0). The cocrystal structure reveals a common configuration of inhibitors binding to the PDE5. Thus, the inhibitors are first embedded in the pocket formed by highly conserved hydrophobic residues, and then, the formation of H-bond with the invariant glutamine controls the orientation of inhibitor binding.

Further, the performance of SABRE$^{Lig-Rec}$ approach was compared to four other methods reported by Vainio et al.,[30] using exactly the same sets of actives and decoys for each target

dx.doi.org/10.1021/ci4005496 | J. Chem. Inf. Model. 2014, 54, 338−346

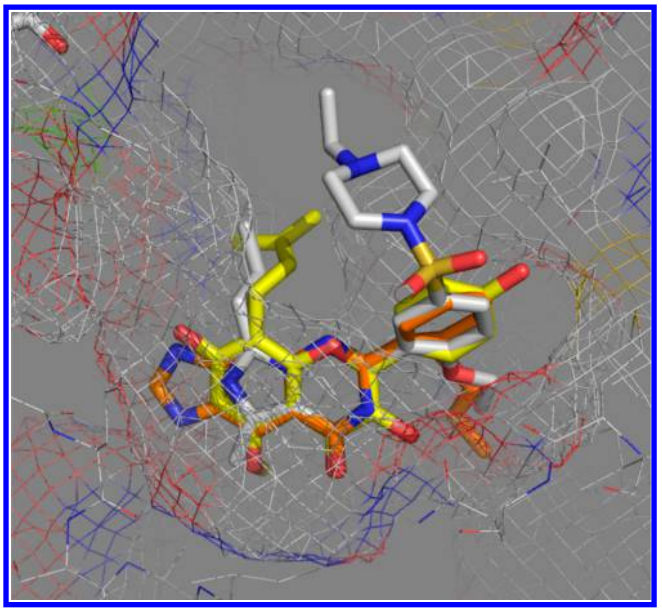

Figure 2. Predicted binding pose of two active compounds (brown ZINC04199930 and yellow ZINC04199939) in the human PDE5 (PDB: 1XP0) active site. The structure of the query (Vardenafil) is displayed in white.

(Table 2). We observe that the overall performance of the ShaEP, ROCS, CF, and FieldScreen methods was less than ⟨AUC⟩ ∼ 0.70, and it seems that none of these tools performs consistently with higher accuracy than the others. The template structures used for some biological targets in the DUD benchmark are obviously inappropriate because these tools produced AUC values close to 0.5, which would be obtained by a random ranking of the compounds. Some AUC values are close to zero, which indicates that the template is better at picking inactive molecules than active ones. One of the advantages of the SABRE approach is that the consensus shape-based approach depends less on the screened targets, as already observed in our previous benchmark test using the 40 DUD targets.[12b,c] This assessment did not cover the whole spectrum of crystal ligand−target complexes reported in the DUD database (40 targets), so it may be risky to draw absolute conclusions about the performance of these programs. SABRE tool should not be limited to only recognize and rank specific bioactive scaffold classes above inactive decoys. The recognition of a wide variety of structurally different ligand classes is an important and desired quality, which should be a good indicator for the chance to successfully identify new hits by virtual screening.

In order to ensure a more rigorous performance comparison of the two different weighted shape-based approaches implemented in SABRE and WEGA tools, we conducted the benchmark test on the 40 targets of DUD database as described by Yan et al.,[19] using the enhanced shape-based screen SABRE^{Lig} program. The query molecules for screening were selected according to the exact procedures presented in teh work of Kirchmair et al.[11a] The average ⟨AUC⟩ value of the best performing query for the 40 DUD targets using SABRE^{Lig} and WEGA methods was 0.92 ± 0.05 and 0.83 ± 0.15, respectively. SABRE^{Lig} method was able to rank the screening results as *excellent* for 82.5% of the 40 DUD targets (33 targets out of 40 have AUC ≥ 0.90). In addition, SABRE^{Lig} method did not fail for any of the screened 40 targets, while the virtual screening results using the combo scoring function computed by WEGA method failed (AUC < 0.6) for alr2 (AUC = 0.51), Hivrt (AUC = 0.41), and pde5 (AUC = 0.50) (Figure 3 and Table SI.1 in the Supporting Information). WEGA gave the best performance for seven of the 40 targets, however, it appears unable to maintain this level of performance across all targets. These results demonstrate that the performance of the weighted Gaussian algorithm WEGA is strongly influenced by the choice of the target. In comparison, the performance of SABRE^{Lig} method was also less sensitive to the choice of the target. These data clearly show that the weighted-shape based screening strategy implemented in both SABRE^{Lig} and SABRE$^{Lig-Rec}$ programs provide excellent virtual screening performances for the 40 studied targets.

Consistency of SABRE Method. To further analyze the consistency of our approach, the screening test of each DUD target was realized for multiple times using different sets of template structures. Thus, the performance and robustness of SABRE$^{Lig-Rec}$ measured by the area under the ROC curve (AUC value) clearly indicate a noticeable correlation to the choice of the known inhibitors in the template. The lowest AUC value obtained for each screened target using SABRE$^{Lig-Rec}$ method is presented in Table 2. We observe that the average ⟨AUC⟩ of the best performing set of five active ligands (AUC = 0.82) is significantly higher (∼29%) compared to the average ⟨AUC⟩ value of the worst performing set of active ligands (AUC = 0.63).

These results suggest that the observed differences between the worst (Table 2, data in comma) and the best AUC values

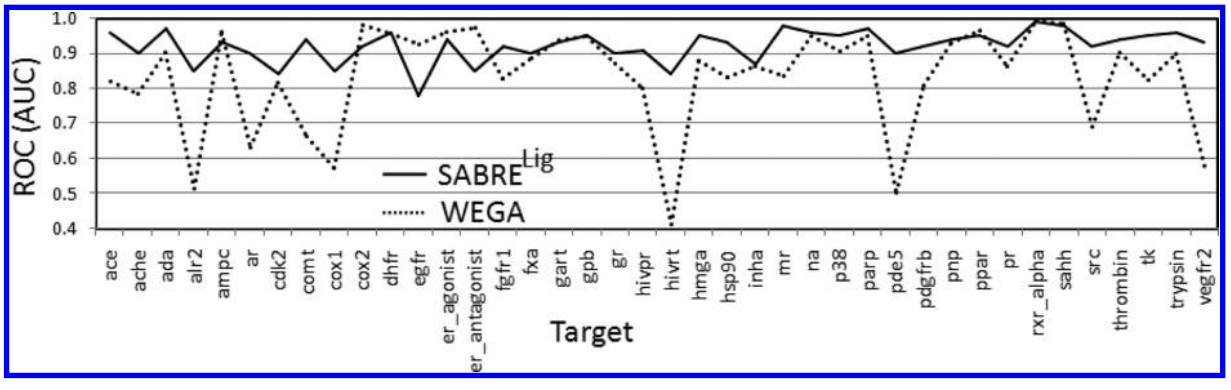

Figure 3. Areas under the ROC curves (AUC) for the 40 targets of the DUD database using SABRE^{Lig} method in comparison with the previously published data using WEGA.[19]

dx.doi.org/10.1021/ci4005496 | J. Chem. Inf. Model. 2014, 54, 338−346

Table 3. Enrichment Factor EF at Top 0.1% and 1% of Database-2 Using Different Virtual Screening Methods

target	$SABRE^{Lig-Rec}$ 0.1%	$SABRE^{Lig-Rec}$ 1%	Glide[a] 1%	Phase[a] 1%	ROCS[a] 1%	EON[a] 1%
ACE	100.0	100.0	30.6	42.9	59.2	63.3
AChE	90.0	99.0	3.8	2.9	69.5	68.6
COX-2	30.0	100.0	52.6	52.0	72.1	35.9
EGFr	20.0	100.0	5.0	70.5	76.4	25.7
FXa	60.0	99.0	54.2	1.1	4.9	1.4
HIVRT	100.0	100.0	10.0	20.0	17.5	17.5
InhA	100.0	91.7	31.8	42.3	49.4	28.2
P38MAP	40.0	100.0	0.4	12.1	7.8	6.6
PDE5	100.0	100.0	2.0	17.7	17.7	9.8
SRC	50.0	100.0	8.4	0.6	0.0	0.0
average	**69.0**	**98.7**	**19.9**	**26.2**	**37.5**	**25.7**
stand. dev.	32.4	2.6	20.9	24.3	30.7	24.3

[a]Reference 27.

may reflect significant differences in the precomputed coefficients of the shape-density model.[12c] Indeed, candidate structures that are similar in shape (but with different scaffold) and pharmacophoric groups composition to an arbitrarily selected query and set of active ligands would have a higher probability to be selected as active hits, whereas the candidate active molecules that significantly differ in shape and functional groups from the reference structures (query + set of active structures) would likely be missing. As described in the Methods section, the optimal coefficients of eq 4 were determined by overlapping the query structure with the template set of known active ligands which characterize the "signature" or "consensus molecular-shape pattern" of active ligands for a specific target. Thus, if the precomputed coefficients are different from those of the candidate active structures of the database, then SABRE algorithm fail to perform an accurate ranking.

These initial tests are encouraging and two conclusions may be drawn from these results. First, in the present study the templates of active ligands were randomly chosen, which may have caused a suboptimal performance of SABRE. It is clear that a judicious choice of the template set of active ligands (for example by increasing the number of active ligands and/or considering the structural diversity of the ligands) will further improve the performance of the virtual screening.

The second conclusion that can be drawn from the tests is the efficiency of data fusion method used with diverse sets of precomputed coefficients of eq 4. It is pretty important for the context of scaffold hopping. Indeed, the set of active ligands can be clustered into several chemotype subsets and the optimal coefficients computed for each subset. Then, the coefficients of each subset can be used for virtual screening and the final results obtained using the data fusion technique.

Analysis of the Enrichment Factor of $SABRE^{Lig-Rec}$ Method. The efficiency of $SABRE^{Lig-Rec}$ method was analyzed using the enrichment factor (EF) and compared to GLIDE, phase, ROCS, and EON.[27] The EF values at the top 0.1% and 1% of the data set describe the early enrichment (Table 3), whereas the EF values at the top 10% represent the late-stage database screening (Table 4). To consider a real-life virtual screening test, we conducted the benchmark test with database-**2** (95 000 decoys) using the same virtual screening protocol and compare our results with those from the literature.[27] The enrichment factor $EF^{1\%}$ and $EF^{10\%}$ using database-**1** are presented in Table SI-2 of the Supporting Information.

Table 4. Enrichment Factor EF at Top 10% of Database-2 Using Different Virtual Screening Methods

target	$SABRE^{Lig-Rec}$	Glide[a]	Phase[a]	ROCS[a]	EON[a]
ACE	10.0	6.1	6.9	7.1	9.6
AChE	9.9	5.1	1.0	7.7	8.1
COX-2	10.0	8.6	7.0	8.7	6.8
EGFr	10.0	4.7	9.0	9.1	5.2
fXa	9.9	8.2	0.9	1.3	0.2
HIVRT	10.0	5.0	3.5	2.8	3.3
InhA	9.2	4.1	4.9	5.3	3.4
P38	10.0	1.6	1.4	1.6	2.1
PDE5	10.0	0.4	3.5	2.6	2.0
SRC	10.0	2.1	0.7	0.5	0.6
average	**9.9**	**4.6**	**3.9**	**4.7**	**4.1**
stand. dev.	0.2	2.7	3.0	3.3	3.2

[a]Reference 27.

The results show that the virtual screening of 7 targets out of 10 reached the maximum enrichment at $EF^{1\%}$ and $EF^{10\%}$, while the targets AchE, fXa, and InhA obtained an enrichment $EF^{1\%}$ superior to 90%. In addition, the data indicates that the $SABRE^{Lig-Rec}$ method never failed for any target, i.e., $EF^{1\%} \neq 0$; whereas, the reported data fusion using multiple virtual screening methods failed to identify active ligands for the SRC target at the top 1% of the database.[27]

An important requirement for a robust virtual screening protocol is that it must rank most of the active ligands very early in a large database, as it is the proportion of the compounds most likely be tested experimentally. We note that the early enrichment of $EF^{1\%}$ corresponds to the top ~950 structures of the database and is beyond the number of compounds to be tested. Then, we computed the enrichment EF at 0.1% corresponding to the top 95 structures of the database-**2**. Surprisingly, $SABRE^{Lig-Rec}$ reached the maximum enrichment factor for five targets (ACE, HIVRT, InhA, and pde5) and the lowest $EF^{0.1\%}$ of 20.0 was obtained for the EGFr target. The screening using $SABRE^{Lig-Rec}$ method achieved an average $EF^{0.1\%}$ and $EF^{1\%}$ of 69.0 ± 32.4 and 98.7 ± 2.6, respectively. These values are compared to the results obtained by Svensson et al. using five different data fusion algorithms.[27] Interestingly, they found that for the 10 DUD targets there is no single data fusion method that consistently would be the best choice, but rather, there are large differences between the data sets. The best average $EF^{1\%}$ value of 41.6 ± 26.0 was obtained using the data fusion with a "rank vote" algorithm.[27]

dx.doi.org/10.1021/ci4005496 | J. Chem. Inf. Model. 2014, 54, 338−346

These results lead us to conclude that the ligand/structure based virtual screening method of SABRE can provide high early enrichment factor when using a large size of ligand database. The outcome of the trials detailed above was unexpected. It seems that the naïve approach of assigning exactly equal weights to the shape of pharmacophoric groups is unjustified. Here, we demonstrate that the variation of the weighting coefficients of the enhanced 3D shape model provides superior performance in virtual screening.

CONCLUSION

We have presented an efficient weighted-shape-based virtual screening approach combining our previous ligand shape-based similarity algorithm and the shape of the protein receptor. The specific point of our approach exploits the pharmacological preferences of a number of known active ligands to take advantage of the structural and chemical similarities using a linear combination of weighted molecular shape-density of the pharmacophorics groups.

The performance of SABRE algorithm was validated using the DUD database. Screening results revealed that SABRE$^{Lig-Rec}$ method is more robust to represent the active ligands with diverse shape structures. The screening stages of a large database showed that SABRE$^{Lig-Rec}$ algorithm outperforms the virtual screening which uses the data fusion of multi screening methods and demonstrates a superior early retrieval rate of active compounds.

The most important characteristic of SABRE is that the performance is dependent upon the amount of information provided by the template of known active ligands. Clearly, if there is a large amount of information (compounds structurally diverse in the template list), then the efficiency of the method to distinguish actives from decoys will also be high. Further efforts integrating our developed ligand/structure shape-based screening method and a database of optimal coefficients for each protein target may be useful in virtual screening of selective and broad spectrum inhibitors with therapeutic activities across multiple diseases (chemogenomics approach).

ASSOCIATED CONTENT

Supporting Information

Detailed information about the enrichment factor at top 1% and 10%, and the ROC (AUC) values for the 40 DUD targets using the SABRE program. This material is available free of charge via the Internet at http://pubs.acs.org.

AUTHOR INFORMATION

Corresponding Author

*E-mail: ahamz3@uky.edu.

Notes

The authors declare no competing financial interest.

REFERENCES

(1) (a) John, S.; Thangapandian, S.; Sakkiah, S.; Lee, K. W. Discovery of potential pancreatic cholesterol esterase inhibitors using pharmacophore modelling, virtual screening, and optimization studies. *J. Enzyme Inhib. Med. Chem.* **2011**, *26* (4), 535−545. (b) Bi, J.; Yang, H.; Yan, H.; Song, R.; Fan, J. Knowledge-based virtual screening of HLA-A*0201-restricted CD8(+) T-cell epitope peptides from herpes simplex virus genome. *J. Theor. Biol.* **2011**, *281* (1), 133−139. (c) Akula, N.; Zheng, H.; Han, F. Q.; Wang, N. Discovery of novel SecA inhibitors of Candidatus Liberibacter asiaticus by structure based design. *Bioorg. Med. Chem. Lett.* **2011**, *21* (14), 4183−4188. (d) Englebienne, P.; Moitessier, N. Docking Ligands into Flexible and Solvated Macromolecules. 4. Are Popular Scoring Functions Accurate for this Class of Proteins? *J. Chem. Inf. Model.* **2009**, *49* (6), 1568−1580. (e) Bleicher, K. H.; Green, L. G.; Martin, R. E.; Rogers-Evans, M. Ligand identification for G-protein-coupled receptors: a lead generation perspective. *Curr. Opin. Chem. Biol.* **2004**, *8* (3), 287−296.

(2) (a) Good, A. C.; Krystek, S. R.; Mason, J. S. High-throughput and virtual screening: core lead discovery technologies move towards integration. *Drug Discovery Today* **2000**, *5* (12), S61−S69. (b) Patel, Y.; Gillet, V. J.; Bravi, G.; Leach, A. R. A comparison of the pharmacophore identification programs: Catalyst, DISCO and GASP. *J. Comput.-Aided Mol. Des.* **2002**, *16* (8−9), 653−681. (c) Schneider, G.; Bohm, H. J. Virtual screening and fast automated docking methods. *Drug Discovery Today* **2002**, *7* (1), 64−70. (d) Bissantz, C.; Folkers, G.; Rognan, D. Protein-based virtual screening of chemical databases. 1. Evaluation of different docking/scoring combinations. *J. Med. Chem.* **2000**, *43* (25), 4759−4767.

(3) (a) Brooijmans, N.; Kuntz, I. D. Molecular recognition and docking algorithms. *Annu. Rev. Biophys. Biomol. Struct.* **2003**, *32*, 335−373. (b) Kitchen, D. B.; Decornez, H.; Furr, J. R.; Bajorath, J. Docking and scoring in virtual screening for drug discovery: Methods and applications. *Nat. Rev. Drug Discovery* **2004**, *3* (11), 935−949. (c) Totrov, M.; Abagyan, R. Flexible ligand docking to multiple receptor conformations: a practical alternative. *Curr. Opin. Struct. Biol.* **2008**, *18* (2), 178−184.

(4) (a) Cheng, T.; Li, Q.; Zhou, Z.; Wang, Y.; Bryant, S. H. Structure-Based Virtual Screening for Drug Discovery: a Problem-Centric Review. *Aaps J.* **2012**, *14* (1), 133−141. (b) Scior, T.; Bender, A.; Tresadern, G.; Medina-Franco, J. L.; Martinez-Mayorga, K.; Langer, T.; Cuanalo-Contreras, K.; Agrafiotis, D. K. Recognizing Pitfalls in Virtual Screening: A Critical Review. *J. Chem. Inf. Model.* **2012**, *52* (4), 867−881.

(5) Lee, H. S.; Choi, J.; Kufareva, I.; Abagyan, R.; Filikov, A.; Yang, Y.; Yoon, S. Optimization of high throughput virtual screening by combining shape-matching and docking methods. *J. Chem. Inf. Model.* **2008**, *48* (3), 489−497.

(6) (a) Schierz, A. C. Virtual screening of bioassay data. *J. Cheminf.* **2009**, *1*, No. 21. (b) Seal, A.; Passi, A.; Jaleel, U. C. A.; Wild, D. J. In-silico predictive mutagenicity model generation using supervised learning approaches. *J. Cheminf.* **2012**, *4*, No. 10.

(7) (a) Willett, P. Similarity-based virtual screening using 2D fingerprints. *Drug Discovery Today* **2006**, *11* (23−24), 1046−1053. (b) Maggiora, G. M.; Shanmugasundaram, V. Molecular Similarity Measures. In *Chemoinformatics and Computational Chemical Biology*; Bajorath, J., Ed.; Springer, 2011; Vol. *672*, pp 39−100. (c) Rouvray, D. H. Predicting Chemistry from Topology. *Sci. Am.* **1986**, *255* (3), 40−. (d) Randic, M. Characterization of Molecular Branching. *J. Am. Chem. Soc.* **1975**, *97* (23), 6609−6615. (e) Randic, M. Nonempirical Approach to Structure Activity Studies. *Int. J. Quantum Chem.* **1984**, 137−153. (f) Vasilescu, D.; Viani, R. Molecular Similarity in Aminothiol Radioprotectors−a Randic Graph Approach. *Int. J. Quantum Chem.* **1987**, 149−165.

(8) (a) Durrant, J. D.; Friedman, A. J.; McCammon, J. A. CrystalDock: A Novel Approach to Fragment-Based Drug Design. *J. Chem. Inf. Model.* **2011**, *51* (10), 2573−2580. (b) Sastry, G. M.; Dixon, S. L.; Sherman, W. Rapid Shape-Based Ligand Alignment and Virtual Screening Method Based on Atom/Feature-Pair Similarities and Volume Overlap Scoring. *J. Chem. Inf. Model.* **2011**, *51* (10), 2455−2466. (c) Zhang, Q.; Muegge, I. Scaffold hopping through virtual screening using 2D and 3D similarity descriptors: Ranking, voting, and consensus scoring. *J. Med. Chem.* **2006**, *49* (5), 1536−1548.

(9) Kinnings, S. L.; Jackson, R. M. LigMatch: A Multiple Structure-Based Ligand Matching Method for 3D Virtual Screening. *J. Chem. Inf. Model.* **2009**, *49* (9), 2056−2066.

(10) Hert, J.; Willett, P.; Wilton, D. J.; Acklin, P.; Azzaoui, K.; Jacoby, E.; Schuffenhauer, A. Comparison of topological descriptors for similarity-based virtual screening using multiple bioactive reference structures. *Org. Biomol. Chem.* **2004**, *2* (22), 3256−3266.

(11) (a) Kirchmair, J.; Distinto, S.; Markt, P.; Schuster, D.; Spitzer, G. M.; Liedl, K. R.; Wolber, G. How To Optimize Shape-Based Virtual Screening: Choosing the Right Query and Including Chemical Information. *J. Chem. Inf. Model.* **2009**, *49* (3), 678−692. (b) Hert, J.; Willett, P.; Wilton, D. J.; Acklin, P.; Azzaoui, K.; Jacoby, E.; Schuffenhauer, A. New methods for ligand-based virtual screening: Use of data fusion and machine learning to enhance the effectiveness of similarity searching. *J. Chem. Inf. Model.* **2006**, *46* (2), 462−470. (c) Venkatraman, V.; Perez-Nueno, V. I.; Mavridis, L.; Ritchie, D. W. Comprehensive Comparison of Ligand-Based Virtual Screening Tools Against the DUD Data set Reveals Limitations of Current 3D Methods. *J. Chem. Inf. Model.* **2010**, *50* (12), 2079−2093.

(12) (a) Giganti, D.; Guillemain, H.; Spadoni, J.-L.; Nilges, M.; Zagury, J.-F.; Montes, M. Comparative Evaluation of 3D Virtual Ligand Screening Methods: Impact of the Molecular Alignment on Enrichment. *J. Chem. Inf. Model.* **2010**, *50* (6), 992−1004. (b) Hamza, A.; Wei, N. N.; Zhan, C. G. Ligand-Based Virtual Screening Approach Using a New Scoring Function. *J. Chem. Inf. Model.* **2012**, *52* (4), 963−974. (c) Hamza, A.; Wei, N.-N.; Hao, C.; Xiu, Z.; Zhan, C.-G. A novel and efficient ligand-based virtual screening approach using the HWZ scoring function and an enhanced shape-density model. *J. Biomol. Struct. Dyn.* **2012**, 1−15.

(13) (a) Zhou, M.; Hamza, A.; Zhan, C.-G.; Thorson, J. S. Assessing the Regioselectivity of OleD-Catalyzed Glycosylation with a Diverse Set of Acceptors. *J. Nat. Prod.* **2013**, *76* (2), 279−286. (b) Zhang, W.; Sviripa, V.; Chen, X.; Shi, J.; Yu, T.; Hamza, A.; Ward, N. D.; Kril, L. M.; Vander Kooi, C. W.; Zhan, C.-G.; Evers, B. M.; Watt, D. S.; Liu, C. Fluorinated N,N-Dialkylaminostilbenes Repress Colon Cancer by Targeting Methionine S-Adenosyltransferase 2A. *ACS Chem. Biol.* **2013**, *8*, 796−803. (c) Stambouli, N.; Dridi, M.; Wei, N.-N.; Jlizi, A.; Bouraoui, A.; Elgaaied, A. B. A. Structural insight into the binding complex: β-arrestin/CCR5 complex. *J. Biomol. Struct. Dyn.* **2013**, 1−10. (d) Zhou, M.; Hou, Y.; Hamza, A.; Zhan, C.-G.; Bugni, T. S.; Thorson, J. S. Probing the Regiospecificity of Enzyme-Catalyzed Steroid Glycosylation. *Org. Lett.* **2012**, *14* (21), 5424−5427. (e) Nejla, S.; Ning-Ning, W.; Asma, J.; Samah, A.; Rim, A.; Baderredine, K.; Amine, S.; Hanen, T. B. A.; Mahdi, D.; Hamza, A.; Amel, B. A. E. Structural insight into a novel human CCR5-V130I variant associated with resistance to HIV-1 infection. *J. Biomol. Struct. Dyn.* **2013**, 1−9.

(14) Jahn, A.; Hinselmann, G.; Nikolas Fechner, N.; Zell, A. Optimal assignment methods for ligand-based virtual screening. *J. Cheminf.* **2009**, *1* (14), 1−23.

(15) (a) Grant, J. A.; Pickup, B. T. A Gaussian Description of Molecular Shape. *J. Phys. Chem.* **1995**, *99* (11), 3503−3510. (b) Grant, J. A.; Gallardo, M. A.; Pickup, B. T. A fast method of molecular shape comparison: A simple application of a Gaussian description of molecular shape. *J. Comput. Chem.* **1996**, *17* (14), 1653−1666.

(16) (a) Mezey, P. G. Topological Shape-Analysis of Chain Molecules—An Application of the GSTE Principle. *J. Math. Chem.* **1993**, *12* (1−4), 365−373. (b) Walker, P. D.; Arteca, G. A.; Mezey, P. G. A Complete Shape Characterization for Molecular Charge-Densities Represented by Gaussian-Type Functions. *J. Comput. Chem.* **1991**, *12* (2), 220−230.

(17) Grant, J. A.; Pickup, B. T. A gaussian description of molecular shape (vol 99, pg 3505, 1995). *J. Phys. Chem.* **1996**, *100* (6), 2456−2456.

(18) (a) Korhonen, S. P.; Tuppurainen, K.; Laatikainen, R.; Perakyla, M. FLUFF-BALL, a template-based grid-independent superposition and QSAR technique: Validation using a benchmark steroid data set. *J. Chem. Inf. Comput. Sci.* **2003**, *43* (6), 1780−1793. (b) Labute, P.; Williams, C.; Feher, M.; Sourial, E.; Schmidt, J. M. Flexible alignment of small molecules. *J. Med. Chem.* **2001**, *44* (10), 1483−1490. (c) Lemmen, C.; Lengauer, T.; Klebe, G. FLEXS: A method for fast flexible ligand superposition. *J. Med. Chem.* **1998**, *41* (23), 4502−4520.

(19) Yan, X.; Li, J.; Liu, Z.; Zheng, M.; Ge, H.; Xu, J. Enhancing Molecular Shape Comparison by Weighted Gaussian Functions. *J. Chem. Inf. Model.* **2013**, *53* (8), 1967−1978.

(20) McGann, M. R.; Almond, H. R.; Nicholls, A.; Grant, J. A.; Brown, F. K. Gaussian docking functions. *Biopolymers* **2003**, *68* (1), 76−90.

(21) (a) Nissink, J. W. M.; Murray, C.; Hartshorn, M.; Verdonk, M. L.; Cole, J. C.; Taylor, R. A new test set for validating predictions of protein-ligand interaction. *Proteins−Structure Function Genetics* **2002**, *49* (4), 457−471. (b) Hartshorn, M. J.; Verdonk, M. L.; Chessari, G.; Brewerton, S. C.; Mooij, W. T. M.; Mortenson, P. N.; Murray, C. W. Diverse, high-quality test set for the validation of protein-ligand docking performance. *J. Med. Chem.* **2007**, *50* (4), 726−741.

(22) (a) Huang, N.; Shoichet, B. K.; Irwin, J. J. Benchmarking sets for molecular docking. *J. Med. Chem.* **2006**, *49* (23), 6789−6801. (b) Cross, J. B.; Thompson, D. C.; Rai, B. K.; Baber, J. C.; Fan, K. Y.; Hu, Y.; Humblet, C. Comparison of Several Molecular Docking Programs: Pose Prediction and Virtual Screening Accuracy. *J. Chem. Inf. Model.* **2009**, *49* (6), 1455−1474.

(23) Cross, J. B.; Thompson, D. C.; Rai, B. K.; Baber, J. C.; Fan, K. Y.; Hu, Y. B.; Humblet, C. Comparison of Several Molecular Docking Programs: Pose Prediction and Virtual Screening Accuracy. *J. Chem. Inf. Model.* **2009**, *49* (6), 1455−1474.

(24) Good, A. C.; Oprea, T. I. Optimization of CAMD techniques 3. Virtual screening enrichment studies: a help or hindrance in tool selection? *J. Comput.-Aided Mol. Des.* **2008**, *22* (3−4), 169−178.

(25) Cheeseright, T. J.; Mackey, M. D.; Melville, J. L.; Vinter, J. G. FieldScreen: Virtual Screening Using Molecular Fields. Application to the DUD Data Set. *J. Chem. Inf. Model.* **2008**, *48* (11), 2108−2117.

(26) Kalliokoski, T.; Salo, H. S.; Lahtela-Kakkonen, M.; Poso, A. The Effect of Ligand-Based Tautomer and Protomer Prediction on Structure-Based Virtual Screening. *J. Chem. Inf. Model.* **2009**, *49* (12), 2742−2748.

(27) Svensson, F.; Karlen, A.; Skold, C. Virtual Screening Data Fusion Using Both Structure- and Ligand-Based Methods. *J. Chem. Inf. Model.* **2012**, *52* (1), 225−232.

(28) (a) Jacobsson, M.; Liden, P.; Stjernschantz, E.; Bostrom, H.; Norinder, U. Improving structure-based virtual screening by multivariate analysis of scoring data. *J. Med. Chem.* **2003**, *46* (26), 5781−5789. (b) Hecker, E. A.; Duraiswami, C.; Andrea, T. A.; Diller, D. J. Use of catalyst pharmacophore models for screening of large combinatorial libraries. *J. Chem. Inf. Comput. Sci.* **2002**, *42* (5), 1204−1211. (c) Diller, D. J.; Li, R. X. Kinases, homology models, and high throughput docking. *J. Med. Chem.* **2003**, *46* (22), 4638−4647.

(29) Triballeau, N.; Acher, F.; Brabet, I.; Pin, J. P.; Bertrand, H. O. Virtual screening workflow development guided by the "receiver operating characteristic" curve approach. Application to high-throughput docking on metabotropic glutamate receptor subtype 4. *J. Med. Chem.* **2005**, *48* (7), 2534−2547.

(30) Vainio, M. J.; Puranen, J. S.; Johnson, M. S. ShaEP: Molecular Overlay Based on Shape and Electrostatic Potential. *J. Chem. Inf. Model.* **2009**, *49* (2), 492−502.